NME 2024 July 28-31, 2024 Xi'an, China

NME1510

# ON THE MICROSTRUCTURE AND DIFFUSION TRANSFORMATION OF PRECIPITATION-HARDENED STERLING SILVER FOR JEWELRY APPLICATION

**Pornnapha Denjarukul[1]*, Sawitchaya Sinpromma[2], Adiruj Peerawat[2], Thanut Jintakosol[2], Chayankittipat Yongperakul[3] and Kageeporn Wongpreedee[2]**

[1]Innovation and Industrial Management Program, College of Creative Industry, Srinakharinwirot University, Bangkok, 10110, Thailand
[2]College of Creative Industry, Srinakharinwirot University, Bangkok, 10110, Thailand
[3]Suparno Jewelry Co., Ltd., Ramkhamhaeng Road, Saphan Sung, Bangkok, 10240, Thailand
*pornnapha.ars@gmail.com

## INTRODUCTION

Sterling silver is an alloy used for demi-fine jewelry, which is in high demand due to the high price of gold jewelry. It contains a minimum of 92.5% pure silver by weight, while the remaining 7.5 wt% alloys are limited to other metals. Silver is a soft metal. Various methods are employed to improve the mechanical properties of sterling silver, such as adjusting the proportions or adding alloying elements like copper to increase its hardness. However, excessive addition of copper may lead to the formation of copper oxides and cause issues in industrial applications.

In this work, the commercial silver alloy at a higher quality level, such as anti-tarnish and formability, with less copper contents must be discovered due to customers' needs for demi-fine jewelry. The researcher designed the percent of silver at various compositions, starting from sterling silver 92.5 wt%, 93.5 wt%, and 94.5 wt%. Common addition alloys like Cu, Ni, and Zn were added to investigate the properties of alloys. The heat treatment processes and results were analyzed, aiming for high-quality and functional jewelry pieces.

## Experimental

### Materials

The induction vacuum-casting machine is used to cast the alloys at three compositions. The alloy's chemical composition is confirmed after casting using X-ray Fluorescence (XRF)

**Ag-Cu system** (Standard Sterling Silver)

**1) Alloy SA** 92.5 %Ag-7.5 %Cu

**Ag-Cu-Zn-Ni System**

**2) Alloy A** 93.5%Ag-5.01%Cu-0.79%Zn-0.70%Ni

**3) Alloy B** 94.5%Ag-4.24%Cu-0.63%Zn-0.63%Ni

### Hardness Test

The mechanical properties of metals will be tested by hardness using a Micro Vickers Hardness Tester at 100 gram-force (HV0.1) for 10 seconds, and the average hardness value will be calculated from 5 points per specimen.

### Precipitation Hardening

The homogeneous solid solution samples were prepared by heating the samples in a Carbolite tube furnace at a temperature of 750 °C for 30 minutes.

Then, the sample was aging at 250 °C, 350 °C, and 450 °C for 5-180 minutes. Finally, rapidly cool the sample by immersing it in water to stop the grain growth of the microstructure.

### Fuming test ($H_2S$ atmosphere)

Tarnishing was carried out by exposing the silver polishing sheet samples to a sulfur vapor environment according to the UNE-EN-ISO 4538 standard. The fuming test was conducted in a closed environment with a 0.4 %$H_2S$ exposure. The samples were covered by sulfur gas for 30 minutes and then characterized using a UV-visible Spectrophotometer for color measurements

The reaction is governed by the following equation.

$$K_2S(s) + 2HCl(aq) \longrightarrow 2KCl(s) + H_2S(g) \quad (1)$$

## Results and discussion

Figure 1 shows the hardness variation from 68 HV- 73 HV, a standard range of as-cast sterling silver. It is noted that a higher silver composition of alloy B at 94.5 wt%Ag, resulting lower hardness of alloys. After the homogenous solid solution process, the hardness of all samples was reduced in the range of 55 HV- 62 HV, as shown in Figure 2, due to the second phase being annihilated and homogenized into the matrix.

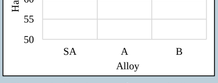


**Figure 1**. Hardness of as-cast alloys.

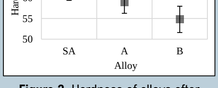


**Figure 2**. Hardness of alloys after homogenization.

Figure 3 shows the homogeneous microstructure of AgCu and AgCuZnNi systems, which are examples of alloy SA and alloy A, respectively. The SE microstructure images show the second phase in Figure 3 a) and b) revealing Cu-phase and c) and d) displaying Cu and Ni-rich second phases at different shapes. However, it is only partially homogenized due to the setting time of 30 minutes for the commercial process. In Figure 3 a) and b), standard alloy SA shows the disintegration of Cu showing second phases. Figures 3 c) and d) show that Cu dissolved in the matrix and annihilated. Alloy A shows less in the second phase of Cu, scattering as second phases into the matrix. It shows the forming of a single Ag-rich phase due to the lower Cu content of alloy A than alloy SA.

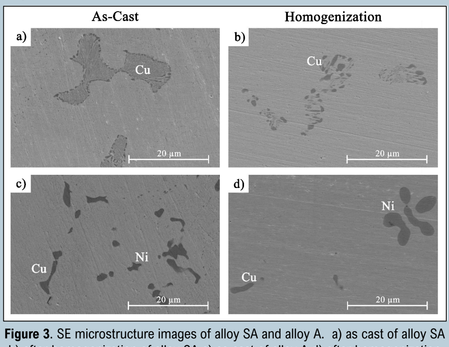


**Figure 3**. SE microstructure images of alloy SA and alloy A. a) as cast of alloy SA b) after homogenization of alloy SA c) as cast of alloy A d) after homogenization of alloy A

Figure 4 displays the hardness graph at various aging times and alloy SA, alloy A, and alloy B temperatures. Alloy SA has a complete precipitation cycle of aging at all temperatures; however, alloy A and alloy B at 250 °C have not developed full GP2 zones. For this reason, precipitation hardening of alloy SA shows outstanding hardness as expected due to the classical binary phase diagram of homogeneous solid solution and aging alloys. This hardness data of aged hardening is consistent with the previous research, which is around 120-160 HV. The maximum hardness of alloy SA is 161.4 ±2.4 HV at 250 °C for 60 minutes. The maximum hardness of alloy A and alloy B are 108.2 ±4.2 HV at 450 °C for 30 minutes and 119.7 ±7.4 HV at 350 °C for 60 minutes, respectively. It is noted that alloy B has higher hardness than alloy A at a maximum range of precipitation hardening, even though there is a higher percentage of Ag at 94.5wt%.

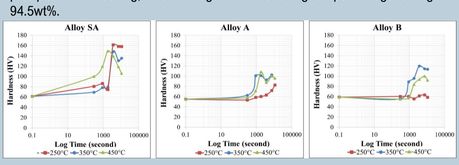


Figure 4. The graph of hardness vs. aging time of alloy SA, alloy A, and alloy B

SE microstructure images also confirm the phenomena of copper segregations, as shown in Figure 5. Alloy SA shows the Cu-rich phases precipitating all over the samples in Figure 5$a_2$ of an SE image and Figure 5$a_3$ of a mapping image. The higher hardness of sample SA, maximum at 161.4 ±2.4 HV, is due to the dislocation barrier along the grain boundaries spread out most areas in the samples. Alloy B shows the best maximum hardness of the precipitation hardening process at 119.7 ±7.4 HV. The higher hardness of alloy B compared to alloy A is due to the segregation of the dislocation barrier of Cu on the boundary of Ni, causing slightly higher hardness. As shown in Figure 5$c_3$, the Ni-rich second phase is wrapped with Cu precipitate along grain boundaries. Alloy A shows the only Ni-rich segregation of the second phase in the sample, giving the maximum hardness of 108.2 ±4.2 HV.

In contrast, no Cu-wrapped Ni second phase exists in alloy A, as shown in Figure 5$b_3$. There is some Cu precipitation as second phases on alloy A; however, the amount of second phases is not high enough to generate the hardness of the sample compared to alloy SA and alloy B. Moreover, alloy A has a higher amount of Zn, which is mostly annihilated into the matrix, and less activation energy to precipitate out, resulting in less hardness.

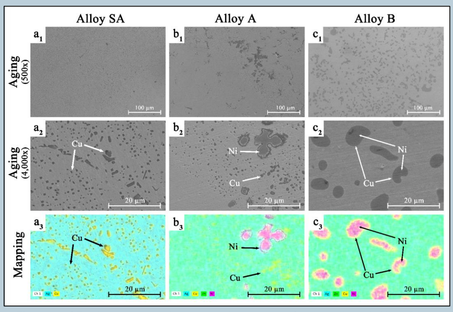


**Figure 5**. SE microstructure images and mapping of aging alloy. a) Alloy SA shows the segregation of Cu second phase b) Alloy A shows Ni second phase precipitated and cu scattering into the matrix c) Alloy B Ni second phase precipitate and cu phase wrap

Figure 6 shows the CIELAB Color Coordinates for the Alloys before and after the $H_2S$ atmosphere test. It was found that the brightest is alloy B, and the darkest is alloy SA. And it was found that the reddest is alloy A. Therefore, in the $H_2S$ atmosphere test, the alloy B was the least tarnished. The L* value, which represents brightness, indicates that alloy B has a significant advantage due to minimal deviation before and after L*. The standard alloy SA shows a high deviation towards darker shades. Additionally, the images in Figure 7, sample sheets after tarnish tests, demonstrate a higher tarnish reaction on the standard alloy SA.

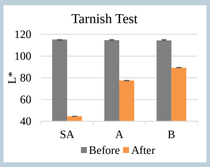


**Figure 6**. Results of CIE L*a*b* test comparison before and after tarnish test of alloy SA, alloy A, and alloy B

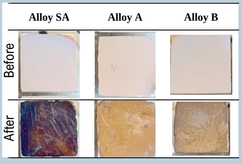


**Figure 7**. Alloy SA, alloy A and alloy B sheets before and after tarnish test.

## Summary

In commercial applications, it is crucial to reduce the copper proportion and increase the number of additional elements while maintaining hardness values. In this experiment, we tested three alloy compositions and developed suitable processes for enhancing hardness properties through three compositions: standard alloy (92.5wt%Ag-7.5wt%Cu), alloy A (93.5wt%Ag-5.01wt%Cu-0.79wt%Zn-0.70wt%Ni), and alloy B (94.5wt%Ag-4.24wt%Cu-0.63wt%Zn-0.63wt%Ni). Two composition alloys of alloy A and alloy B fix Cu content at 77.08 wt% and vary Zn and Ni at 12.15wt%Zn-10.77wt%Ni for alloy A and 77.09wt%Cu-11.45wt%Zn-11.45wt%Ni for alloy B. This process of altering the alloy composition and heat treatment is key to enhancing hardness properties.

After the heat treatment, the results demonstrated a substantial increase in overall hardness, from 60-70 HV to 120-160 HV. This finding underscores the importance of the alloy composition and heat treatment process. The precipitation hardening process and composition of Alloy B proved superior to that of Alloy A.

The SEM micrograph provides a visual representation of the unique microstructure of Alloy B, which features a higher Ni-rich second phase precipitated and wrapped with the Cu phase along the grain boundary. This unique microstructure is the key to Alloy B having higher hardness than Alloy A. With a high percentage of Ag composition at 94.5 wt% and less Cu content, Alloy B achieved an optimum hardness of precipitation hardening at 119.7± 7.4 HV at 350 °C at 60 minutes, along with better tarnish resistance. Therefore, Alloy B achieved an optimum hardness of precipitation hardening at 119.7± 7.4 HV at 350 °C at 60 minutes, along with better tarnish resistance.

## References

[1] K. Wongpreedee, Advanced Jewelry Casting Technology. Bangkok: Srinakharinwirot University. (2008)
[2] G. Rayhitsaum, Sterling Silver- U.S. Patent Review, The 28th Santa Fe Symposium on Jewelry Manufacturing Technology. (2014)
[3] S. Sakultanchareoncha, T. Chairuangsri and E. Nisaratanaporn, Microstructure and Mechanical Properties of As-cast and Heat-treated 935AgCuSnSi Alloys, Chiang Mai J. Sci., vol. 43, 2016, pp. 206-214.
[4] G. E. Gardam, Sterling silver containing aluminuum, Metallurgia., vol. 47(279), 1998, pp. 29-33.
[5] J. T. Strauss, Tarnish-proof sterling: understanding the limitations, The 22nd Santa Fe Symposium on Jewelry Manufacturing Technology., 2008, pp. 307-326.
[6] E. Nisaratanaporn, S. Wongsriruksa, S. Pongsukiwat and G. Lothongkum, Study on the microstructure, mechanical properties, tarnish and corrosion resistance of Sterling silver alloyed with manganese, Materials Sciences and Engineering A., 2007, pp. 445-446: 663-668.
[7] Y. Qingqing, X. Weihao, Y. Zhen, S. Dingjie and W. Ronghui, Corrosion and tarnish behaviour of 925Ag75Cu and 925Ag40Cu35Zn alloys in synthetic sweat and H2S atmosphere, Rare Met.Mater., vol. 39(4), 2010, pp. 578-581.
[8] S. Dimitrijević, V. Parezanin, Z. Kamberović, M. Ranitovic, M. Korac and S. Dimitrijevic, Design of anti-tarnish sterling silver Ag-Cu-Zn alloy and investigation of silicon addition influence on mechanical and corrosion characteristics, Chemical Industry and Chemical Engineering Quarterly., 2018, pp. 38-38.
[9] A. Yanil, P. Visuttipitukul, E. Nisaratanaporn and C. Preuksarattanawut, Effects of Indium and Gallium ratio on tarnish resistance, corrosion and mechanical properties of 950 silver alloy, J Met Mater Miner., vol. 33, no. 1, pp. 39–46, (2023)
[10] J. R. Butler, U.S. Patent 10,697,044 B1. (2020)
[11] S. Praiphrukˌ G. Lothongkum, E. Nisaratanaporn and B. Lohwongwatana, Investigation of supersaturated silver alloys for high hardness jewelry application, J. Met. Mater. Miner., vol. 23, no 2. (2013)
[12] M. Grimwade, Heat Treatment of Precious Metals and Their Alloys, The Fifth Santa Fe Symposium on Jewelry Manufacturing Technology. (1991)
[13] B. Lohwongwatana, P. Wirot, C. Yiyvintum, A. Khamkongkaeo, C. Puncreobutr, G. Lothongkum, E. Nisaratanaporn and T. E. Vichaidith, Comparative Test for Identification of Silver Tarnishing, Proceeding of the Fifth Santa Fe Symposium on Jewelry Manufacturing Technology. (2015)